RAPID TOOLING BY INTEGRATING ELECTROFORMING AND SOLID FREEFORM FABRICATION TECHNIQUES

Bo Yang **Ming C. Leu***

Department of Mechanical Engineering
New Jersey Institute of Technology
Newark, New Jersey 07102
Tel: 973-596-5668, Fax: 973-596-5601, E-mail: bxy0487@oak.njit.edu

Abstract: This paper describes a rapid tooling process that integrates solid freeform fabrication (SFF) with electroforming to produce metal tools including molds, dies, and electrical discharge machining (EDM) electrodes. Based on experimental data analysis, the geometry and material of the SFF part, the properties of the electroformed metal, and the process parameters are significant factors that cause inaccuracy in the manufactured tools. Thermomechanical modeling and numerical simulation is used to determine the geometry of the SFF part and the electroform thickness for minimizing the manufacturing time and cost while satisfying the tooling accuracy requirement.

Keywords: Solid freeform fabrication, Rapid tooling, Electroforming, Mold, EDM electrode, Finite element analysis.

1. INTRODUCTION

Solid freeform fabrication (SFF), or rapid prototyping (RP), is being increasingly used in industry for prototyping, tooling and manufacturing applications [1, 2]. Rapid tooling is the process of directly or indirectly employing RP technologies to fabricate castings, dies, molds and EDM electrodes. Currently used rapid hard tooling processes such as 3D Keltool™ [3], 3-dimensional printing (3DP) [4] and RapidTool™ [5], first bind metal powders by various techniques to generate a green part. Afterwards the part is debinded, sintered, and infiltrated with copper or other metals to produce functional metal parts. The powder metallurgy approaches involve random noise shrinkage during the sintering process and thus the generated metal parts suffer dimensional uncertainty and they usually have rough surface finish.

Electroforming is the use of electrodeposition of metal onto a part that is subsequently separated from the deposit to produce a metal shell. This can be used to make molds and dies for replicating the part [6]. The metalized part, which has the required shape, dimensions, accuracy and roughness, is sinked into an electrolyte bath as the cathode and deposited a layer of metal, normally copper or nickel, for a specified thickness. The part is then separated from the metal shell. The shell is then backed with other materials to form a mold cavity or an EDM electrode. A nickel electroformed part can be used for a prototyping tool or even a production tool [7], and a

* Dr. Ming C. Leu is on leave at the National Science Foundation as the Program Director for Manufacturing Machines and Equipment.

copper electroformed part can be used as an EDM electrode [8]. Metals deposited by electroforming have distinct properties [9]. Dimensional tolerances can be very good, often up to 0.0025 mm, and surface finishes of 0.05 μm and better can be obtained quite readily if the master part is adequately smooth [10]. The emergence of rapid prototyping technology has brought about new opportunities for electroforming in rapid production tooling. Since electroforming can closely copy the geometry and surface quality of an RP part, the accuracy and surface finish of the produced tool is largely determined by the accuracy and surface finish of the RP part.

This paper first describes the tooling process and case studies on electroforming of SL parts to generate EDM electrodes and mold cavities. The investigation on the tooling generation demonstrates that the main sources of tooling inaccuracy are thermal deformations caused by burning out the SL part and by backfilling the electroformed metal shell with a molten metal. At the process of separating the metal shell from the SL part, the part is incinerated at about 560 °C. The thermal expansion of the SL part deforms the metal shell because the coefficient of thermal expansion of the SL part material is much larger than that of nickel or copper. In the backfilling process, the molten metal is cast into a metal box and solidified, which also generates thermal deformation. Only low melting alloy (melts below 135 °C) is used in the case studies so that the backfilling deformation is not serious.

A thermomechanical model is established to analyze the thermally induced stress during the burnout of the SL part. The model is implemented in ANSYS software to numerically simulate the thermal stress based on finite element method (FEM). The analysis demonstrates that appropriate geometry design of the RP part and appropriate electroform thickness not only reduce thermal stress thus improving tooling accuracy, but also minimize manufacturing time and cost. The presented study demonstrates that the integration of electroforming with solid freeform fabrication is a viable way for the making of metal dies, molds, and EDM electrodes.

2. TOOLING PROCESS AND CASE STUDIES

2.1 Tooling Process

The process for making EDM electrodes using SL parts and electroforming is illustrated in Fig.1. Compared with making EDM electrodes by direct electroplating of copper on positive SL parts [11], this method does not require uniform thickness of the plated copper. The negative (complementary) geometry of the EDM electrode is prototyped by stereolithography for use as the RP part. The part must be rigid enough to withstand the electroforming stress [12] induced during the metal layer deposition. Before electroforming of the SL part, metalization of the SL surface is needed to make the part electrically conductive. Several techniques for metalization of nonconductive materials are available [13]. Electroless plating, a process involving autocatalytic or chemical reduction of aqueous metal ions onto a base substrate, is used to metalize the SL part. The metalized SL parts are then electroplated with copper to a desired thickness. In the process of separating the SL part from the metal shell, prevention of the electroform deformation is extremely important. The RP part built with ceramic and other difficult-to-melt materials are

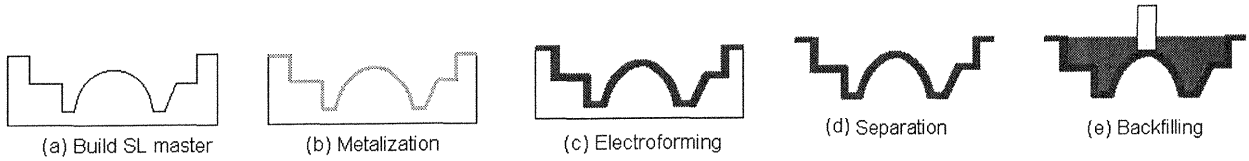

Figure 1. EDM tooling process

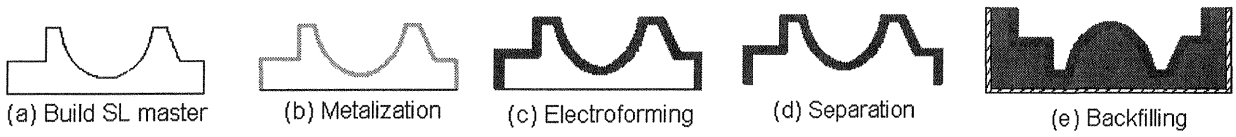

Figure 2. Mold tooling process.

preferred to be separated by mechanical extraction. Melting, burning out, or heat softening can be applied to wax and thermoplastic RP parts. SL resin is a thermosetting material, and burning out of the SL part is the preferred separation method. Complete incineration of the SL part is observed at the temperature of about 560 °C. During the burnout process, the heat results in expansion of the part. This may crack or deform the electroformed metal shell. The geometry of the RP part and the thickness of the electroformed metal shell needs to be optimized in order to minimize the manufacturing cost, while the stresses exerted on the metal shell due to the thermal expansion of the part do not crack the copper shell or generate unacceptable deformation. Because the EDM electrode does not contact the workpiece during the electrical discharge machining process, the strength of the electrode is not critical. A low melting alloy with good electrical and thermal conductivity is good for backfilling the shell to form an EDM electrode.

The rapid mold making process is very similar to the process for making EDM electrodes. This is illustrated in Fig.2. A layer of metal, which is thick enough to resist the deformation caused by the separation and backfilling, is electroformed upon an SL part metalized by nickel electroless plating. The deformation of the metal shell generated during the burnout process is largely affected by the electroforming thickness, material properties and the geometry of the part. Backfilling of the electroform is more critical in manufacturing a mold cavity compared with manufacturing an electrode due to the high strength required in the subsequent injection molding process. The harder the backfilled metal, the higher the strength of the mold cavity. However, a harder metal usually has a higher melting temperature. Casting with a high melting temperature metal tends to generate larger thermal stresses, which may cause larger deformation in the electroformed metal shell. To reduce the injection molding cycle time, conformal cooling lines may be put around the nickel shell before the backfilling process.

2.2 Case Studies

Two SL parts of the same geometry, as illustrated in Fig.3(a), are used to make EDM electrodes using the tooling process with the copper layer thickness of 2 mm and 4 mm. The cavity of the SL part is 12 mm deep. The SL cavities are polished to the surface finish of 1.24 μm. After polishing, key dimensions are measured three times and the average is recorded. After burning out the SL resin at the oven temperature of 560 °C, the corresponding dimensions are measured and compared with the data measured on the SL parts. It is found that the dimensional deviation of the electrode with 4 mm thick copper shell is smaller than that of the electrode with 2 mm thick copper shell. It means that the thinner the copper layer, the lower the dimensional accuracy of the electrode resulted from the burning process. The largest deviation is 0.24% for the 2 mm thick copper layer electrode, and 0.19% for the 4 mm thick one. The surface finish of the two finished EDM electrodes is measured, and the average surface roughness is about 1.26 μm for both electrodes. The copper shell is backed with a tin-lead alloy whose melting point is 103 °C. The finished 2 mm copper layer electrode is then used to machine a hard steel workpiece to a depth of 10 mm in 3 hours and 25 minutes.

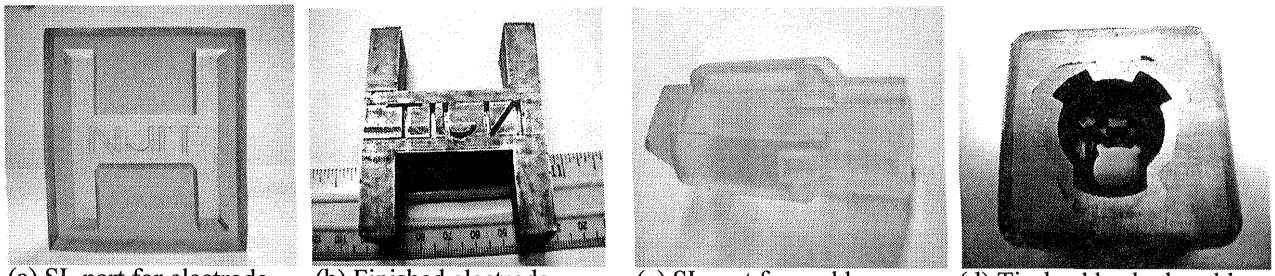

(a) SL part for electrode (b) Finished electrode (c) SL part for mold (d) Tin-lead backed mold

Figure 3: Electroformed electrode and Mold generated by the tooling process.

Two nickel electroformed mold cavities shown in Fig. 3(d) are made by the mold tooling process. Nickel is used in the electroforming because its mechanical properties are about the same as those of stainless steel and nickel is highly wear and corrosion resistant. After metalizing the parts with nickel to a thickness of about 0.005 mm by electroless plating, the parts are nickel-electroformed with sulfamate electrolyte to form nickel shells with the thicknesses of 2 mm and 4 mm. The electroformed SL parts are then put into an oven to burn out the resin at 560 °C. The dimensional deviation of the mold with 2 mm thick nickel is larger than that of the mold with 4 mm thick nickel. The largest deviation is 0.25%. The nickel electroforms are then backfilled with molten tin-lead alloy whose melting temperature is 138.5 °C. The surface finish of both mold cavities is measured about 1.27 μm, which is nearly the same as that of the SL parts.

2.3 Factors Affecting Tooling Accuracy

The factors that affect accuracy in the described tooling process include the accuracy of the RP part, deformation caused by electroforming stress [12], and thermal deformations generated during the separation and backfilling processes. With various techniques, electroforming can achieve deviation between the master part and the electroformed tool as small as 0.0025 mm [10]. Thermal deformations caused by burning out the part and by backfilling the electroformed shell with molten metal thus are important sources of inaccuracy. Low melting point alloys with good electrical and thermal conductivity can be used to backfill the shell to form an EDM electrode with small thermal deformation. An electroformed mold cavity backed with a high-strength metal can significantly improve the durability of the electroformed mold and increase the ability of the mold to resist deformation during the injection molding process. However, a high-strength metal always has a high melting point, which may generate large deformation in the mold cavity when it is solidifying.

3. MODELING AND ANALYSIS OF THE BURNOUT PROCESS

3.1 Thermomechanical Modeling of the Burnout Process

Thermal stresses induced during the burnout of an SL part are a multi-material, non-linear, transient thermal-mechanical coupling problem. Boley and Weiner [14] proved that the thermal solution is independent of any changes caused by thermally-induced stresses under the condition that the time history of displacement closely follows the change of temperature, and vise versa. Assume that the burnout process satisfies the condition beause the thermal expansion closely follows the temperature variation, then the thermomechanical coupling problem can be simplified as an uncoupled, transient thermal stress problem. Under this assumption, the modeling of the thermal stress can be divided into two steps: thermal modeling and structural modeling.

Thermal modeling is used to compute the transient temperature field T(x,y,z,t) during the burnout process. The governing heat conduction equation is

$$\alpha \nabla^2 T = \frac{\partial T}{\partial t} \tag{1}$$

where $\alpha = \frac{k}{c\rho}$, k, c, and ρ are heat conductivity, specific heat, and material density, respectively.

The two initial conditions are that the metal shell and the master are at the room temperature, T_r. Because the hot air inside the oven chamber is in a perfect thermal contact with the outer surface of the electroformed object, the thermal convection effect can be ignored during the burnout process. Thus the first boundary condition is:

$$T(p,t) = f(t) \tag{2}$$

where p is a point on the surface of the metal, and $f(t)$ represents the oven temperature.

Because the metal shell is in perfect contact with the RP part, the heat transfer at the boundary surfaces of the RP part and the metal shell is conduction dominated. So the temperatures at these surfaces are the same. In addition, the heat flux leaving metal shell through the contact surface equals to that entering the RP part. Thus for a point P on the contact surface of the metal and the RP part, the boundary conditions are:

$$T_m(P_b,t) = T_r(P_b,t) \tag{3}$$

$$k_m \frac{\partial T_m}{\partial n}(P_b,t) = k_r \frac{\partial T_r}{\partial n}(P_b,t) \tag{4}$$

where the subscripts m and r refer to the metal shell and the RP material, respectively, and n is the normal to the boundary surface at point P_b.

Structure modeling is used to calculate the thermally-induced stress exerted on the metal shell. The problem of thermoelasticity consists of determining the following:

6 stress components: σ_{xx}, σ_{yy}, σ_{zz}, σ_{xy}, σ_{yz}, σ_{zx},

6 strain components: ε_{xx}, ε_{yy}, ε_{zz}, ε_{xy}, ε_{yz}, ε_{zx}, and

3 displacement components: u, v, w

that need to satisfy the following fifteen equations:

3 equilibrium equations:

$$\left.\begin{aligned} \frac{\partial \sigma_{xx}}{\partial x} + \frac{\partial \sigma_{xy}}{\partial y} + \frac{\partial \sigma_{xz}}{\partial z} = 0 \\ \frac{\partial \sigma_{xy}}{\partial x} + \frac{\partial \sigma_{yy}}{\partial y} + \frac{\partial \sigma_{yz}}{\partial z} = 0 \\ \frac{\partial \sigma_{xz}}{\partial x} + \frac{\partial \sigma_{yz}}{\partial y} + \frac{\partial \sigma_{zz}}{\partial z} = 0 \end{aligned}\right\} \tag{5}$$

6 stress-strain relations:

$$\left.\begin{aligned} \varepsilon_x = \frac{1}{E}[\sigma_{xx} - \upsilon(\sigma_{yy} + \sigma_{zz})] + e \cdot \nabla T \\ \varepsilon_y = \frac{1}{E}[\sigma_{yy} - \upsilon(\sigma_{xx} + \sigma_{zz})] + e \cdot \nabla T \\ \varepsilon_z = \frac{1}{E}[\sigma_{zz} - \upsilon(\sigma_{yy} + \sigma_{xx})] + e \cdot \nabla T \\ \gamma_{xy} = \frac{1}{2G}\sigma_{xy}; \gamma_{yz} = \frac{1}{2G}\sigma_{yz}; \gamma_{zx} = \frac{1}{2G}\sigma_{zx} \end{aligned}\right\} \tag{6}$$

and 6 strain-displacement relations:

$$\left.\begin{aligned} \varepsilon_{xx} &= \frac{\partial u}{\partial x}; \quad \varepsilon_{yy} = \frac{\partial v}{\partial y}; \quad \varepsilon_{zz} = \frac{\partial w}{\partial z} \\ \varepsilon_{xy} &= \frac{1}{2}\gamma_{xy} = \frac{1}{2}\left(\frac{\partial v}{\partial x} + \frac{\partial u}{\partial y}\right) \\ \varepsilon_{yz} &= \frac{1}{2}\gamma_{yz} = \frac{1}{2}\left(\frac{\partial w}{\partial y} + \frac{\partial v}{\partial z}\right) \\ \varepsilon_{zx} &= \frac{1}{2}\gamma_{zx} = \frac{1}{2}\left(\frac{\partial u}{\partial z} + \frac{\partial u}{\partial z}\right) \end{aligned}\right\} \tag{7}$$

where e is the coefficient of thermal expansion, and the shear modulus G is related to Young's modulus E and Poisson's ratio υ by $G = \frac{E}{2(1+\upsilon)}$.

3.2 FEM Based Thermal Stress Computation

The above thermomechanical model is applied to an SL cylinder with the outer radius of 50 mm and length of 100 mm, which is nickel electroformed and then burned. The radius A of the inner hole of the cylinder and the electroform thickness t are variables. We assume that the oven is preheated to the burnout temperature (560 °C) and the temperature is constant during the burning

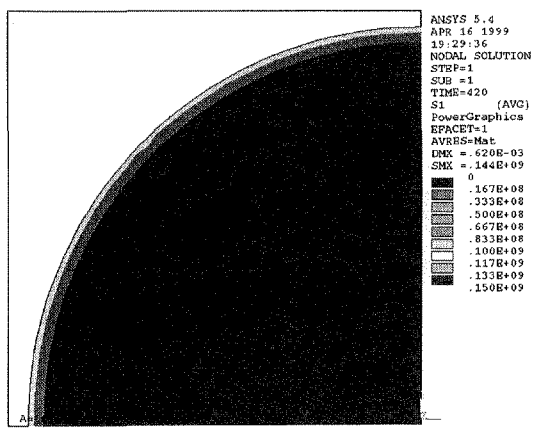

a. SL part with A=0 mm, t=2 mm

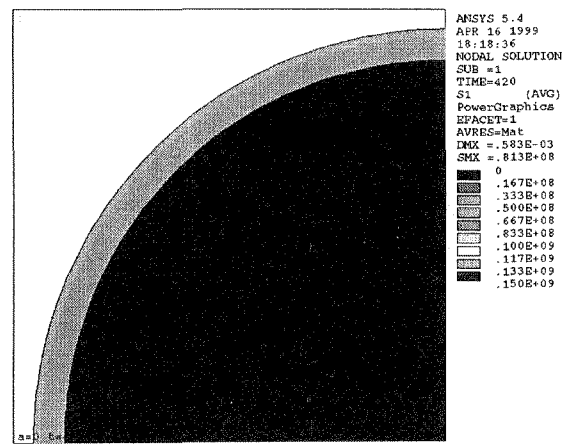

b. SL part with A=0 mm, t=4 mm

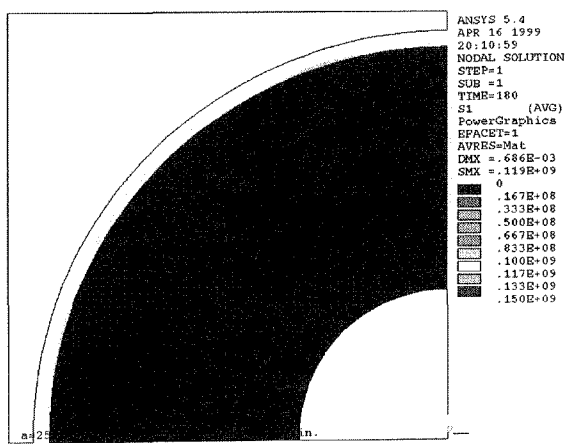

c. SL part with A=25 mm, t=2 mm

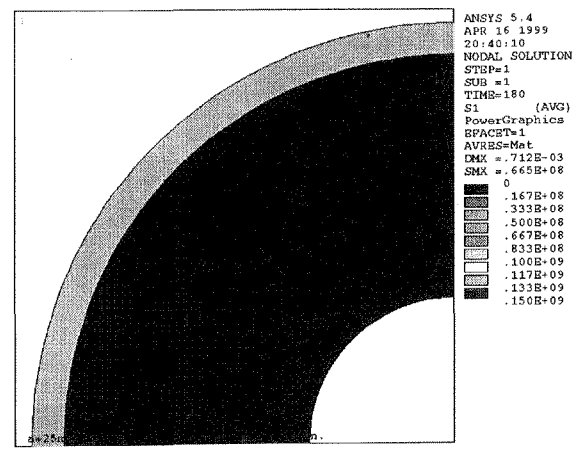

d. SL part with A=25 mm, t=4 mm

Figure 4. Simulation of thermal stresses with different SL parts and electroform thickness

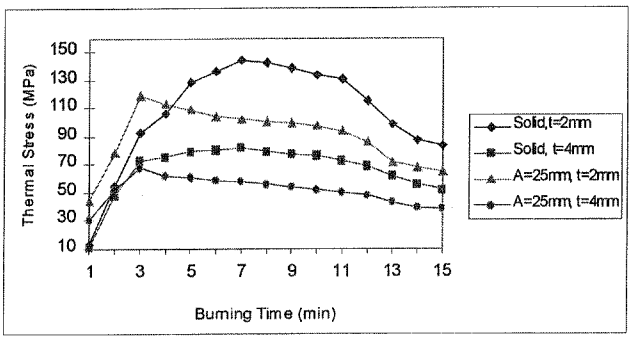

Figure 5. Maximum thermal stress vs. time during burnout process.

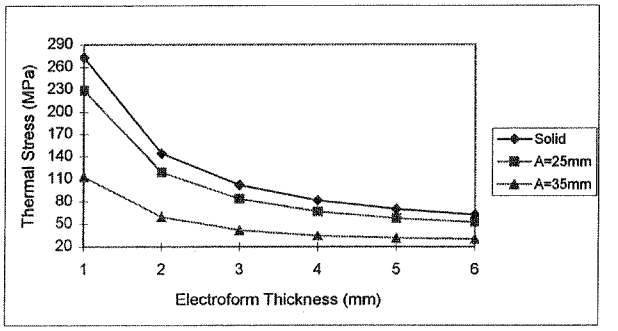

Figure 6. Maximum thermal stress vs. electroform thickness for burnout process.

process. To solve this problem, ANSYS 5.4, a finite element analysis software package, is used to simulate the thermal stress resulted from the burnout process. Fig. 4 shows the simulation results with four different sets of variables. For solid SL parts, when electroform thickness increases from 2 mm to 4 mm, the maximum thermal stress decreases from 144 MPa to 81.3 MPa (see Fig. 4(a) and 4(b)). If A=25 mm, compared with the solid SL parts the maximum thermal stress for 2 mm electroform thickness reduces from 144 MPa to 119 MPa (see Fig. 4(a) and 4(c)), and that for 4 mm electroform thickness reduces from 81.3 MPa to 66.5 MPa (see Fig. 4(b) and 4(d)). During the burnout process, the maximum thermal stress changes over time, as illustrated in Fig.5. Fig.6 illustrates that with the same SL part structure, the maximum thermal stress decreases when electroform thickness increases. The inner hole can always decrease the thermal stress: the larger the hole, the smaller the thermal stress. This demonstrates that thermal stress induced by the burnout process can be reduced when an RP part is built with appropriate design of its structure. The structure needs to be strong enough to resist the electroforming stress, which is determined by electroforming process parameters. In our case, if the electroforming stress exerted on the electroformed nickel shell is 10 MPa, the deformation caused by the electroforming stress can be calculated as is listed in Table 1. From the table, we can see that solid SL parts always have smaller electroforming deformations. When A increases, the electroforming deformation increases. Table 2 lists the build time and material cost for different SL parts. It shows by how much the inner hollow structure can save build time and material cost.

Table 1. Electroforming deformation (ED) for different sets of parameters A and t

	t =1 mm	t =2 mm	T =3 mm	t =4 mm	t =5 mm	t =6 mm
A=0 mm	0.0024	0.0046	0.0067	0.0078	0.0109	0.0128
A=25 mm	0.0043	0.0085	0.0142	0.0187	0.0231	0.0275
A=35 mm	0.0096	0.0194	0.0282	0.0372	0.0461	0.0547

Table 2. Comparison of build time and material cost for different SL parts

	Build Time (hour)	SL 5170 Material Cost
Solid	35.27	$ 161.63
A=25mm	26.46	$ 121.25
A=35mm	17.98	$ 82.43

4. CONCLUSION

The method of solid freeform fabrication combined with electroforming for fabricating metal molds and EDM electrodes is presented. The case studies indicate that the described method is feasible for rapid tooling of molds and EDM electrodes. The electroforming thickness affects the mechanical property and dimensional accuracy of the mold. Thermal deformations caused by burning out the SL part and backfilling the electroformed metal shell with molten metal are identified as the major sources of inaccuracy. The thermomechanical modeling and FEM based numerical simulation of the stress induced during the burnout process is performed. The analysis demonstrates that the structure of the SFF part and the electroform thickness have significant effects on the fabrication time and cost and the tooling accuracy.

5. ACKNOWLEDGMENT

This work is partially supported by the New Jersey Commission on Science and Technology via the Multi-lifecycle Engineering Research Center at New Jersey Institute of Technology.

6. REFERENCES

1. Kruth, J. -P., Leu, M. C., Nakagawa, N., 1998, Progress in Additive Manufacturing and Rapid Prototyping, Annals of the CIRP, 47/2.
2. Leu, M.C. and Zhang, W., 1998, Research and Development of Rapid Prototyping and Tooling in the United States, Proc. of First International Conference on Rapid Prototyping and Manufacturing, Beijing, China.
3. Jacobs, P.F., 1997, Recent Advances in Rapid Tooling from Stereolithography, Proc. of the Seventh International Conference on Rapid Prototyping, San Francisco.
4. Sachs, E., Cima, M., Cornie, J., 1990, Three-Dimensional Printing: Rapid Tooling and Prototyping Directly from a CAD Model, Annals of the CIRP, 39/1/:201-204.
5. Bourell, D.l., Crawford, R.H., Marcus, H.L., Beaman, J.J., Barlow, J.W., 1994, Selective Laser Sintering of Metals, J. of Manufacturing Science and Engineering, 68/2:519-527.
6. Spiro, P., 1968, Electroforming, Robert Draper Ltd.
7. Yang, B., Leu, Ming C., 1999, Integration of Rapid Prototyping and Eletroforming for Tooling Application. Annals of the CIRP, 48/1.
8. Yang, B., Leu, Ming C., 2000, EDM Tooling by Electrodeposition of Rapid Prototyping Parts. International Journal of Agile Manufacturing, Vol. 1.
9. Safranek, William H., 1986, The Properties of Electrodeposited Metals and Alloys. Second edition, American Electroplaters and Surface Finishers Society, Orlando, Florida.
10. Degarmo, E.P., Black, J.T., Kohser, R.A., 1984, Materials and Processes in Manufacturing, Sixth edition, Macmillan Publishing Company, New York.
11. Leu, M.C., Yang B., Yao, W.L., 1998, A Feasibility Study of EDM Tooling Using Metalized Stereolithography Models. Technical Papers of NAMRC, XXVI, Atlanta.
12. Stein, B., 1996, A Practical Guide to Understanding, Measuring and Controlling Stress in Electroformed Metals, Proc. of AESF Electroforming Symposium, Las Vegas.
13. Duffy, J. I., 1980, Electroless and Other Non-Electrolytic Plating Techniques, Noyes Data Corporation, New Jersey.
14. Boley, Bruno A., Weiner, Jerome H., 1960, Theory of Thermal Stresses, John Wiley &Sons, New York.